

Supporting Material

Long-Time Bacterial Diffusivity of a 3-Step Swimmer

Here we provide an alternative derivation of bacterial diffusivity for 3-step swimmers. Let the bacterium displacement per swimming cycle ($\Delta_{CCW} + \Delta_{CW}$) be \vec{r}_i . The total displacement after N cycles is simply $\vec{R}_N = \sum \vec{r}_i$. If there is no directional correlation between \vec{r}_i 's, the mean square displacement is given by $\langle \vec{R}_N \cdot \vec{R}_N \rangle = Na^2$, where $a^2 \equiv \langle |\vec{r}_i|^2 \rangle$. This is a general result applicable to 2-step as well as 3-step swimmers. For the 2-step swimmer, the motility is produced only during the CCW intervals and hence $a^2 = v^2 \langle \Delta_{CCW}^2 \rangle = 2v^2 \tau_{CCW}^2$, where $\tau_{CCW} = \langle \Delta_{CCW} \rangle$ and the PDF $P(\Delta_{CCW})$ is exponential. For the 3-step swimmer, both forward and backward intervals produce motility and hence the mean square displacement during one cycle is given by $a^2 = v^2 \langle \delta^2 \rangle$, where $\delta = |\Delta_{CCW} - \Delta_{CW}|$. If both Δ_{CCW} and Δ_{CW} are exponentially distributed, $\langle \Delta_{CCW} \rangle = \tau_{CCW}$ and $\langle \Delta_{CW} \rangle = \tau_{CW}$, and if there is no correlation between Δ_{CCW} and Δ_{CW} in a swimming cycle, the PDF of δ is

$$P(\delta) = \frac{1}{\tau_{CCW} + \tau_{CW}} \left[\exp\left(-\frac{\delta}{\tau_{CCW}}\right) + \exp\left(-\frac{\delta}{\tau_{CW}}\right) \right]. \quad (\text{S1})$$

Below we make the simplifying assumption $\tau_{CCW} \approx \tau_{CW}$, which yields $a^2 = 2v^2 \tau_{CCW}^2$. To complete the calculation, we notice that $N \approx t / \langle \Delta_{CCW} \rangle = t / \tau_{CCW}$ for 2-step swimmers and $N = t / (\langle \Delta_{CCW} \rangle + \langle \Delta_{CW} \rangle) = t / (2\tau_{CCW})$ for 3-step swimmers, where t is the swimming

time. In d -dimensional space, the bacterial diffusivity D is defined as,

$$\langle \vec{R}_N \cdot \vec{R}_N \rangle = 2dDt, \quad (\text{S2})$$

which gives rise to $D = v^2\tau_{CCW}/d$ for the 2-step swimmers and $D = v^2\tau_{CCW}/(2d)$ for the 3-step swimmers. In one dimension, $d = 1$, the result is consistent with what we derived for the master equations using $\delta J_{CW} = 0$. However, if we use the alternative sorting, assuming $\delta J_{CCW} = 0$, the bacterial diffusivity D is inconsistent with the above calculation.

Conditions of Detailed Balance in the Moving Frame of Swimming Bacteria

In the moving frame of bacteria, the steady state condition requires $\frac{d}{dt} \dots \equiv (\frac{\partial}{\partial t} \pm v \cdot \frac{\partial}{\partial x}) \dots = 0$.

It follows from Eqs. 10-13 in the main text that the following conditions must be satisfied:

$P_{CW}(\hat{x}, x, t) = P_{CCW}(\hat{x}, x, t)$, $P_{CCW}(-\hat{x}, x, t) = \frac{k_0 - \Delta k}{k_0 + \Delta k} P_{CCW}(\hat{x}, x, t)$, and $P_{CW}(-\hat{x}, x, t) = \frac{k_0 - \Delta k}{k_0 + \Delta k} P_{CCW}(\hat{x}, x, t)$. This yields $P_{CW}(x, t) (\equiv P_{CW}(\hat{x}, x, t) + P_{CW}(-\hat{x}, x, t)) = \frac{2k_0}{k_0 + \Delta k} P_{CCW}(\hat{x}, x, t)$

and $\Delta P_{CW}(x, t) (\equiv P_{CW}(\hat{x}, x, t) - P_{CW}(-\hat{x}, x, t)) = \frac{2\Delta k}{k_0 + \Delta k} P_{CCW}(\hat{x}, x, t)$. The above relations show (i) $J_{CW} (\equiv v\Delta P_{CW}) \propto \Delta k$ and (ii) $\delta J_{CW} = J_{CW} - v\frac{\Delta k}{k_0} P_{CW}$ vanishes faster than Δk . Physically, δJ_{CW} is a measure of the deviation from detail balance, and when $\Delta k/k_0 \ll 1$, it can be ignored.

The Discretized Versions of the Master Equations and Their Numerical Solutions

Discretized versions of the master equations for the 2-step and 3-step swimmer are developed below, and they are used for the numerical calculations. In the continuum limit these equations are consistent with those in the main text, Eqs. 3-4 and Eqs. 10-13. All of our

computations were done with Matlab (The MathWorks).

We divided space into segments of equal size Δx located at $\{x_i\}$, and divided time into equal intervals Δt at $\{t_i\}$. For the 2-step case, the conservation of probability demands,

$$P(\hat{x}, x_i, t_i) = P(\hat{x}, x_{i-1}, t_{i-1}) - \frac{1}{2}(k_0 - \Delta k(x_i)) \Delta t P(\hat{x}, x_{i-1}, t_{i-1}) + \frac{1}{2}(k_0 + \Delta k(x_i)) \Delta t P(-\hat{x}, x_{i+1}, t_{i-1}), \quad (\text{S3})$$

$$P(-\hat{x}, x_i, t_i) = P(-\hat{x}, x_{i+1}, t_{i-1}) - \frac{1}{2}(k_0 + \Delta k(x_i)) \Delta t P(-\hat{x}, x_{i+1}, t_{i-1}) + \frac{1}{2}(k_0 - \Delta k(x_i)) \Delta t P(\hat{x}, x_{i-1}, t_{i-1}). \quad (\text{S4})$$

Physically, $P(\hat{x}, x_i, t_i)$ (or $P(-\hat{x}, x_i, t_i)$) is the probability of finding a cell swimming in \hat{x} (or $-\hat{x}$) direction at x_i and t_i . If a cell reaches x_i at time t_i , it must be either at x_{i-1} swimming along the \hat{x} direction or at x_{i+1} swimming along the $-\hat{x}$ direction at time t_{i-1} . Among cells arriving from x_{i-1} , which is $P(\hat{x}, x_{i-1}, t_{i-1})$, $1 - (k_0 - \Delta k(x_i))\Delta t$ of them will continue in the current swimming direction \hat{x} , and $(k_0 - \Delta k(x_i))\Delta t$ of them will randomize their swimming direction. Upon direction randomization, 50% of the this sub-population swims in \hat{x} and the other 50% in $-\hat{x}$ direction. Together, $1 - \frac{1}{2}(k_0 - \Delta k(x_i))\Delta t$ of $P(\hat{x}, x_{i-1}, t_{i-1})$ contributes to $P(\hat{x}, x_i, t_i)$, which corresponds to the first two terms in Eq. S3. Likewise, the same argument shows that $\frac{1}{2}(k_0 + \Delta k(x_i))\Delta t$ of $P(-\hat{x}, x_{i+1}, t_{i-1})$ also contributes to $P(\hat{x}, x_i, t_i)$, which corresponds to the last term in Eq. S3. Similar conservation equations can be derived for the sub-population $P(-\hat{x}, x_i, t_i)$, yielding Eq. S4. Expanding terms in the above equations around x_i and t_i , we recovered the continuous master equations, Eqs. 3-4, in the limits $\Delta x \rightarrow 0$, $\Delta t \rightarrow 0$, and $\Delta x/\Delta t \rightarrow v$.

The derivation for the 3-step case is more tedious, but the idea is the same. The four

equations are given by,

$$\begin{aligned}
P_{CCW}(\hat{x}, x_i, t_i) &= [1 - (k_0 - \Delta k(x_i)) \Delta t] P_{CCW}(\hat{x}, x_{i-1}, t_{i-1}) \\
&\quad + \frac{1}{2} (k_0 - \Delta k(x_i)) \Delta t P_{CW}(\hat{x}, x_{i-1}, t_{i-1}) \quad , \quad (\text{S5}) \\
&\quad + \frac{1}{2} (k_0 + \Delta k(x_i)) \Delta t P_{CW}(-\hat{x}, x_{i+1}, t_{i-1})
\end{aligned}$$

$$\begin{aligned}
P_{CCW}(-\hat{x}, x_i, t_i) &= [1 - (k_0 + \Delta k(x_i)) \Delta t] P_{CCW}(-\hat{x}, x_{i+1}, t_{i-1}) \\
&\quad + \frac{1}{2} (k_0 + \Delta k(x_i)) \Delta t P_{CW}(-\hat{x}, x_{i+1}, t_{i-1}), \quad (\text{S6}) \\
&\quad + \frac{1}{2} (k_0 - \Delta k(x_i)) \Delta t P_{CW}(\hat{x}, x_{i-1}, t_{i-1})
\end{aligned}$$

$$\begin{aligned}
P_{CW}(\hat{x}, x_i, t_i) &= [1 - (k_0 - \Delta k(x_i)) \Delta t] P_{CW}(\hat{x}, x_{i-1}, t_{i-1}) \\
&\quad + (k_0 + \Delta k(x_i)) \Delta t P_{CCW}(-\hat{x}, x_{i+1}, t_{i-1}) \quad , \quad (\text{S7})
\end{aligned}$$

$$\begin{aligned}
P_{CW}(-\hat{x}, x_i, t_i) &= [1 - (k_0 + \Delta k(x_i)) \Delta t] P_{CW}(-\hat{x}, x_{i+1}, t_{i-1}) \\
&\quad + (k_0 - \Delta k(x_i)) \Delta t P_{CCW}(\hat{x}, x_{i-1}, t_{i-1}). \quad (\text{S8})
\end{aligned}$$

This set of equations is again consistent with Eqs. 10-13 in the continuum limit.

In the calculation, we assigned $\Delta x = 0.1$, $2L = 200$ or $2000\Delta x$, $\Delta t = 1$, and $v = \Delta x/\Delta t = 0.1$. Using the computational step Δt as the basic time unit, we defined the transition rates, $k_0 = 0.1$ and $\Delta k = 0.01$, giving the drift velocity $v_d = v\Delta k/k_0 = 10^{-2}$. The equations are solved using the reflective boundary conditions at $x = \pm L$. To generate the numerical solutions in Fig. 1, Eqs. S3-S4 and Eqs. S5-S8 were solved using the initial conditions $P(\pm\hat{x}, x_i, 0) = \exp(-x_i^2/2\sigma^2)/2\sqrt{2\pi\sigma^2}$ and $P_{CCW}(\pm\hat{x}, x_i, 0) = P_{CW}(\pm\hat{x}, x_i, 0) = \exp(-x_i^2/2\sigma^2)/4\sqrt{2\pi\sigma^2}$, respectively. Here, $\sigma = 5\Delta x$ was used. To obtain the numerical solutions in Fig. 2, the initial conditions $P(\pm\hat{x}, x_i, 0) = 1/(4L/\Delta x)$ and $P_{CCW}(\pm\hat{x}, x_i, 0) = P_{CW}(\pm\hat{x}, x_i, 0) = 1/(8L/\Delta x)$ were used for the 2-step and 3-step swimmers, respectively.

Calculations For an Initially Uniform Bacterial Distribution

In most of laboratory experiments the initial bacterial concentration is uniform and the profile evolves under the influence of an imposed chemical gradient. We therefore extend our calculation in the main text to this useful situation. In one dimension, the bacterial profile at $t = 0$ is given by $P(x, 0) = 1/2L$, and the Fourier coefficients are given by,

$$\begin{cases} A_n = 2q'q_n\psi_{0n}^3 \sinh(q'L) \cos(q_nL), \\ B_m = 2q'q_m\phi_{0m}^3 \cosh(q'L) \sin(q_mL). \end{cases} \quad (\text{S9})$$

The analytical and numerical results are plotted in Fig. S1, where the designations of colored symbols and lines are identical to that of Fig. 1. We noticed that in this case the bacterial profiles develop near the boundaries first and then spread into the interior of the sample. The problem in hand involves multiple length scales, L , q'^{-1} , and $q_{m,n}^{-1}$, and it is useful to know their corresponding time scales in an experiment. Eq. 20 makes it clear that the relaxation rate for the attainment of a quasi-steady state is given by $\lambda_0 = Dq'^2 = v_d^2/4D$. Since $v_d = v(\Delta k/k_0)$ and $D = v^2/(\epsilon k_0)$, we found $\lambda_0 = \frac{\epsilon k_0}{4} \left(\frac{\Delta k}{k_0}\right)^2$, where $\epsilon = 1$ for *E. coli* and $\epsilon = 2$ for *V. alginolyticus*. This indicates that the profile formation time λ_0^{-1} is essentially independent of the bacterial swimming speed v but depends on the switching rate k_0 , the sensitivity characterized by $\Delta k/k_0$, and the motility pattern specified by ϵ . Due to the relatively large system size in a typical experiment or in a natural habitat, $L \gg q'^{-1}$, the drift time L/v_d on the scale of the system size, or for that matter the diffusion time L^2/D , is irrelevant. For a large system, therefore, it is expected that a quasi-steady state with a defined profile develops near the peak of the chemical profile over the time scale λ_0^{-1} . For longer times, $\lambda_0^{-1} < t < L/v_d$, the profile increases in amplitude with its exponential form $\sim \exp(2q'x)$ more-or-less preserved. Our calculation displayed in Fig. S1 is consistent

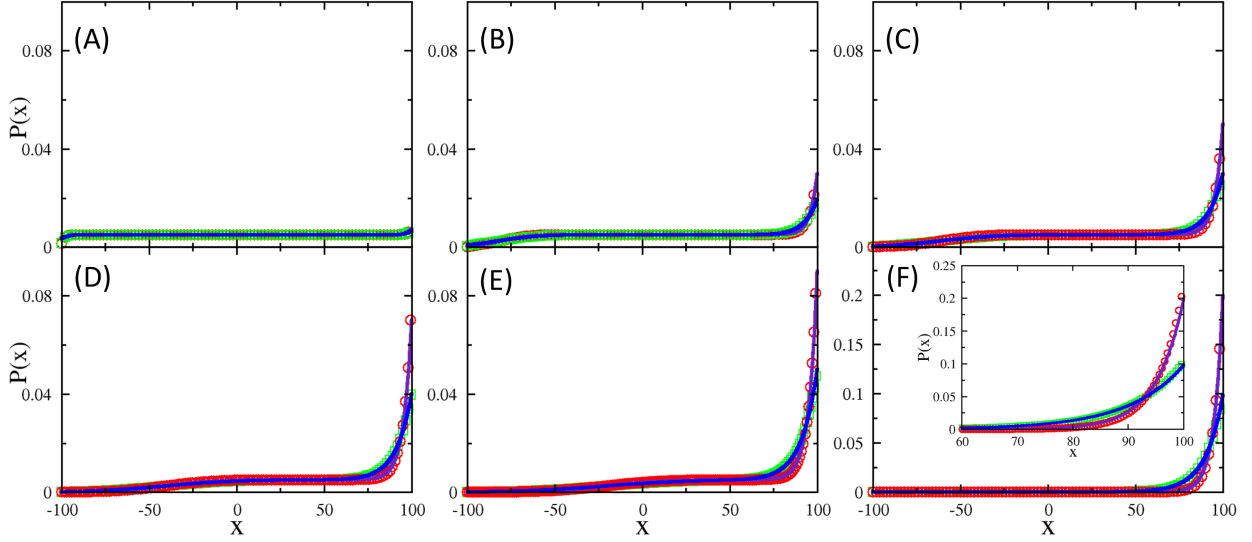


Figure S1: Evolution of $P(x, t)$ starting from the flat distribution $P(x, 0) = 1/2L$ in the presence of a linear chemoattractant gradient in the $+\hat{x}$ direction. The bacterial profiles of the 2-step (blue lines) and 3-step (purple lines) swimmers, calculated based on Eq. 18 at reduced times $t/t_v = 0.01, 0.2, 0.4, 0.6, 0.8,$ and 2 , are plotted in (A-F) respectively. The numerical results based on Eqs. 3-4 and 10-13 are plotted using green squares and red circles for the 2-step and 3-step swimmers. The inset in (F) is the close-up view of the same figure. Note that the shapes of the bacterial profiles near the peak of the chemical concentration $x = L$ form at early t where $t/t_v \ll 1$. Afterward, the peak grows in height but the shapes of the profiles remain more-or-less the same.

with this picture, where $\lambda_0^{-1} = 4000\Delta t$ and $2000\Delta t$ for the 2-step and 3-step swimmer, respectively.

The Memory Effect

Bacteria detect chemical gradients by temporal comparison. Processing of the chemical signals typically introduces a time delay in response. Such a delay in general reduces the drift velocity of the cell. This is because if a cell's swimming direction is reversed at a certain moment, immediately after the reversal, the gradient "computed" by the cell is opposite to the gradient currently experienced by the cell due to the delay (1). For example, if the cell swims up an attractant gradient before it goes down the gradient due to a direction

randomization, within the memory time right after the reversal, dc/dt computed by the cell is still positive. As a result, instead of increasing the switching rate, the cell reduces the switching rate and its average displacement down the gradient is extended. Similarly, right after a cell switches from going down to going up the gradient, its average displacement up the gradient is decreased. The memory effect can be taken into consideration systematically as demonstrated by de Gennes (2). Based on the molecular and functional aspects of *E. coli* chemotaxis (3, 4) and using a linear response, the change in the switching rate Δk depends on the history of chemical exposure and can be mathematically expressed as,

$$\frac{\Delta k(t)}{k_0} = \int_{-\infty}^t R(t-t')c(t')dt'. \quad (\text{S10})$$

In the above, $c(t)$ is the chemical concentration sensed by the bacterium at time t , and $R(t)$ is the response function given by

$$R(t) = R_0 \frac{\tau_Z \tau_m}{\tau_m - \tau_Z} \left(\frac{1}{\tau_Z} \exp(-t/\tau_Z) - \frac{1}{\tau_m} \exp(-t/\tau_m) \right), \quad (\text{S11})$$

where τ_Z and τ_m are respectively the dephosphorylation and methylation times, and R_0 is the amplitude of the response.

For the 2- and 3-step swimmers having the same swimming speed v and the same response $R(t)$, it can be shown using the results in Refs. (1, 2) that the ratio of the drifting velocities for the two bacteria is given by,

$$\frac{v_V}{v_E} = \frac{1}{2} \left(\frac{1}{1 + k_0 \tau_Z} + \frac{1}{1 + k_0 \tau_m} \right). \quad (\text{S12})$$

The effect of memory on bacterial chemotaxis and in particular on the drift velocity have also been considered by Taktikos et. al (5). It was assumed that the chemotactic response function has a typical time scale k_0^{-1} (see Eq. 26 of Ref. (5)). With such an assumption, Eq. S12 yields $v_V \approx \frac{1}{2}v_E$ for $k_0 \tau_Z \approx 1$ and $k_0 \tau_m \approx 1$, which is consistent with Eq. 28 of Ref. (5). Thus, bacterial memory generally makes 3-step swimmers drift slower in a linear chemical

gradient than their 2-step counterparts unless the bacteria can process the chemical signal rapidly with $k_0\tau_Z \ll 1$ and $k_0\tau_m \ll 1$. In this case the drifting velocity of a 3-step swimmer would not be compromised by the delay, and one obtains the result $v_V \approx v_E$.

Supporting References

1. Altindal, T., L. Xie, and X.-L. Wu, 2011. Implications of Three-Step Swimming Patterns in Bacterial Chemotaxis. *Biophys. J.* 100:32–41.
2. de Gennes, P., 2004. Chemotaxis: the role of internal delays. *Eur. Biophys. J.* 33:691–693.
3. Tu, Y., T. Shimizu, and H. Berg, 2008. Modeling the chemotactic response of *Escherichia coli* to time-varying stimuli. *Proc. Natl. Acad. Sci. USA* 105:14855.
4. Celani, A., T. Shimizu, and M. Vergassola, 2011. Molecular and Functional Aspects of Bacterial Chemotaxis. *J. Stat. Phys.* 144:219–240.
5. Taktikos, J., H. Stark, and V. Zaburdaev, 2013. How the Motility Pattern of Bacteria Affects Their Dispersal and Chemotaxis. *PLoS ONE* 8:e81936.